WALAILAK JOURNAL
http://wjst.wu.ac.th Physical Sciences

# Slip Effects on the Unsteady Stagnation Point Flow with Variable Free Stream

**Tasawar HAYAT[1], Sabir Ali SHEHZAD[1,*] and Muhammad QASIM[2]**

[1]*Department of Mathematics, Quaid-i-Azam University, Islamabad 44000, Pakistan*
[2]*Department of Mathematics CIIT, Park Road, Chak Shahzad, Islamabad 44000, Pakistan*

**([*]Corresponding author's e-mail: ali_qau70@yahoo.com)**

*Received: 14 April 2012, Revised: 1 May 2012, Accepted: 29 April 2013*

**Abstract**

We perform a study for the boundary layer flow of viscous fluid about a stagnation point on an unsteady stretching sheet in the presence of variable free stream. Both the velocity and thermal slip conditions are taken into consideration. The stretching velocity and the surface temperature are time-dependent. In the solutions we adopt the homotopy analysis method (HAM). The analysis related to convergence of the solutions is explicitly discussed. The dependence of velocity and temperature profiles on various quantities is discussed by displaying graphs. Comparison of the present solution yields an excellent agreement with an exact solution in a limiting sense.

**Keywords**: Slip conditions, viscous fluid, stretching sheet, stagnation point flow, variable free stream

## Introduction

The boundary layer flows over a stretching surface arise in several engineering processes. The specific examples for practical applications of flows over continuous surfaces include heat-treated materials, travelling between feed roll and a wind up roll, aerodynamic extrusion of plastic sheets, paper production, crystal growing etc. Many researchers have looked at the various aspects of stretching flow problem since the initial study by Sakiadis [1,2]. However much has been stated about stretching flow problems in the steady situations. There are also few studies which deal with such flow problems in the time-dependent case. We only refer some recent studies in this direction [3-8]. The investigation of stretched flow further narrowed down when no-slip condition is not adequate. For example, Mukhopadhyay and Andersson [9] examined the flow and heat transfer over an unsteady stretching surface when both velocity and thermal slip effects are present. Hayat *et al.* [10] also discussed the magnetohydrodynamic (MHD) flow and heat transfer in a fluid bounded by a permeable sheet when no-slip condition is no longer valid. Sharma and Singh [11] analyzed the flow of viscous fluid about a stagnation point on a stretched sheet in the presence of a time-dependent free stream. Zhu *et al.* [12] analyzed the MHD stagnation point flow over a power law stretching sheet in the presence of slip effects. The magnetohydrodynamic flow over a stretched surface with slip condition has been examined by Fang *et al.* [13].

The purpose of current article is to investigate the flow and heat transfer over an unsteady stretching surface in the presence of a time-dependent free stream. Both velocity and thermal slip conditions are considered. The whole arrangement is structured into the 5 sections. Section two contains the mathematical formulation. The series solutions of velocity and temperature by homotopy analysis method (HAM) [14-20] are derived in section three. Discussion of graphs and tables is presented in section four. Section five includes main conclusions.

**Problem formulation**

We consider the Cartesian coordinate system in such a way that the $x-$ axis is chosen along a stretching sheet. The stretching sheet occupies the plane $y=0$ and an incompressible viscous fluid fills the half plane $y>0$. Our interest is to investigate flow in the vicinity of the stagnation point over a stretching surface with partial slip effects. The whole analysis has been carried out in the presence of a time-dependent free stream. The relevant equations are;

$$\frac{\partial u}{\partial x}+\frac{\partial v}{\partial y}=0, \tag{1}$$

$$\frac{\partial u}{\partial t}+u\frac{\partial u}{\partial x}+v\frac{\partial u}{\partial y}=U\frac{\partial U}{\partial x}+\frac{\partial U}{\partial t}+\nu\frac{\partial^2 u}{\partial y^2}, \tag{2}$$

$$\rho C_p\left[\frac{\partial T}{\partial t}+u\frac{\partial T}{\partial x}+v\frac{\partial T}{\partial y}\right]=k\frac{\partial^2 T}{\partial y^2}. \tag{3}$$

In the above expressions $u$ and $v$ denote the velocity components in the $x-$ and $y-$ directions, $T$ is the fluid temperature, $k$ is the thermal conductivity, $C_p$ is the specific heat, $\nu=(\mu/\rho)$ is the kinematic viscosity, $\rho$ is the density of the fluid and $\mu$ is the dynamic viscosity of the fluid. Further note that in Eq. (3), the viscous dissipation effects have been neglected. The boundary conditions for the considered problem are given by;

$$u=U_w+N\mu\frac{\partial u}{\partial y},\ v=0,\ T=T_w+K\frac{\partial T}{\partial y}\ \text{ at } y=0, \tag{4}$$

$$u=U(x,t)=\frac{bx}{1+\alpha t},\ T=T_\infty\ \text{ as } y\to\infty, \tag{5}$$

here $N=N_0(1+\alpha t)^{1/2}$ is the velocity slip factor, $K=K_0(1+\alpha t)^{1/2}$ is the thermal slip factor and for $N=0=K$, the no-slip conditions are recovered. We introduce

$$\eta(y,t)=\left[\frac{c}{\nu(1+\alpha t)}\right]^{1/2}y,\ \psi(x,y,t)=\left[\frac{\nu c}{(1+\alpha t)}\right]^{1/2}xf(\eta),\ \theta=\frac{T-T_\infty}{T_w-T_\infty}, \tag{6}$$

where

$$u=\frac{\partial\psi}{\partial y},\quad v=-\frac{\partial\psi}{\partial x}, \tag{7}$$

with $\psi$ as the stream function. The stretching velocity $U_w(x,t)$ and the surface temperature are taken as;

$$U_w(x,t)=\frac{cx}{1+\alpha t},\ T_w=T_\infty+\frac{1}{(1+\alpha t)^2}. \tag{8}$$

Now Eqs. (2) - (5) yield;

$$f''' + (f + \frac{1}{2}\eta\alpha^*)f'' + (\alpha^* - f')f' + \lambda^2 - \lambda\alpha^* = 0, \tag{9}$$

$$\theta'' + \Pr(f + \frac{1}{2}\eta\alpha^*)\theta' + 2\Pr\alpha^*\theta = 0, \tag{10}$$

$$f = 0,\ \ f' = 1 + S_f f''(0),\ \ \theta = 1 + S_T\theta'(0)\ \ \text{at}\ \eta = 0, \tag{11}$$

$$f' = \lambda,\ \ \theta = 0\ \ \text{at}\ \eta \to \infty,$$

where prime denotes the derivative with respect to $\eta$ and continuity Eq. (1) is identically satisfied, where $\lambda = \frac{b}{c}$ is the ratio of free stream velocity parameter and stretching parameter, $\Pr = \frac{\mu C_p}{\kappa}$ the Prandtl number, $\alpha^* = \frac{a}{c}$ is a parameter, $S_f = N_0\rho\sqrt{a\nu}$ and $S_T = K_0\sqrt{\frac{a}{\nu}}$ are the non-dimensional slip factor and thermal slip parameter, respectively.

The skin-friction coefficient $C_f$ and the local Nusselt number $Nu_x$ are;

$$C_f = \frac{\tau_w}{\rho U_w^2/2},\ \ Nu_x = \frac{xq_w}{k(T_w - T_\infty)}, \tag{12}$$

where the skin-friction $\tau_w$ and heat transfer $q_w$ are;

$$\tau_w = \mu\left(\frac{\partial u}{\partial y}\right)_{y=0},\ q_w = -k\left(\frac{\partial T}{\partial y}\right)_{y=0}. \tag{13}$$

The non-dimensional form of Eq. (13) is;

$$\frac{1}{2}C_f\,\mathrm{Re}_x^{1/2} = f''(0),\ \ Nu/\mathrm{Re}_x^{1/2} = -\theta'(0). \tag{14}$$

**Solution by homotopy analysis method (HAM)**

The velocity $f(\eta)$ and temperature $\theta(\eta)$ with base functions $\{\eta^k\exp(-n\eta), k \geq 0, n \geq 0\}$, Are;

$$f(\eta) = \sum_{n=0}^{\infty}\sum_{k=0}^{\infty} a_{m,n}^k \eta^k \exp(-n\eta), \tag{15}$$

$$\theta(\eta) = \sum_{n=0}^{\infty}\sum_{k=0}^{\infty} b_{m,n}^k \eta^k \exp(-n\eta), \tag{16}$$

where $a_{m,n}^k$ and $b_{m,n}^k$ are the coefficients.

The initial guesses are considered as;

$$f_0(\eta) = \lambda\eta + \frac{(1+\lambda)}{(1+S_f)}\left(1 - e^{-\eta}\right), \tag{17}$$

$$\theta_0(\eta) = \frac{\exp(-\eta)}{1+S_T}, \tag{18}$$

while the following linear operators satisfying the corresponding properties are;

$$L_f = f''' - f', \quad L_\theta = \theta'' - \theta, \tag{19}$$

with

$$L_f(C_1 + C_2 e^{\eta} + C_3 e^{-\eta}) = 0, \;\; L_\theta(C_4 e^{\eta} + C_5 e^{-\eta}) = 0, \tag{20}$$

where $C_i \;\; (i = 1-5)$ are arbitrary constants.

**Zeroth order deformation equations**

Putting the nonlinear operators $\mathbf{N}_f$ and $\mathbf{N}_\theta$ as;

$$\begin{aligned}\mathbf{N}_f[f(\eta,p),\theta(\eta,p)] = {} & \frac{\partial^3 f(\eta,p)}{\partial\eta^3} - \left(f(\eta,p) + \frac{1}{2}\eta\alpha^*\right)\frac{\partial^2 f(\eta,p)}{\partial\eta^2} - \alpha^*\frac{\partial f(\eta,p)}{\partial\eta} \\ & -\left(\frac{\partial f(\eta,p)}{\partial\eta}\right)^2 + \lambda^2 - \lambda\alpha^*,\end{aligned} \tag{21}$$

$$\begin{aligned}\mathbf{N}_\theta[\theta(\eta,p),\mathrm{f}(\eta,p)] = {} & \frac{\partial^2\theta(\eta,p)}{\partial\eta^2} + \Pr\left(\mathrm{f}(\eta,p) + \frac{1}{2}\eta\alpha^*\right)\frac{\partial\theta(\eta,p)}{\partial\eta} \\ & +2\Pr\alpha^*\theta(\eta,p).\end{aligned} \tag{22}$$

The zeroth order problems can be expressed as;

$$(1-p)L_f\left[\hat{f}(\eta;p) - f_0(\eta)\right] = p\hbar_f\mathbf{N}_f\left[\hat{f}(\eta;p),\hat{\theta}(\eta,p)\right], \tag{23}$$

$$(1-p)L_\theta\left[\hat{\theta}(\eta;p) - \theta_0(\eta)\right] = p\hbar_\theta\mathbf{N}_\theta\left[\hat{f}(\eta;p),\hat{\theta}(\eta,p)\right], \tag{24}$$

$$\begin{aligned}&\hat{\mathrm{f}}(0;\mathrm{p}) = \lambda, \; \hat{\mathrm{f}}'(0;\mathrm{p}) = 1 + \mathrm{S_f f''}(0,\mathrm{p}), \\ &\hat{\mathrm{f}}'(\infty;\mathrm{p}) = 0, \; \hat{\theta}(0,\mathrm{p}) = 1 + \mathrm{S_T}\theta'(0,\mathrm{p}), \; \hat{\theta}(\infty,\mathrm{p}) = 0,\end{aligned} \tag{25}$$

where $p$ is an embedding parameter and $\hbar_f$ and $\hbar_\theta$ are the non-zero auxiliary parameters. At $p = 0$ and $p = 1$ we have;

$$\hat{f}(\eta;0) = f_0(\eta), \; \hat{\theta}(\eta,0) = \theta_0(\eta) \text{ and } \hat{f}(\eta;1) = f(\eta), \; \hat{\theta}(\eta,1) = \theta(\eta). \tag{26}$$

We noted that when $p$ changes from 0 to 1 then $f(\eta,p)$ and $\theta(\eta,p)$ vary from $f_0(\eta),\theta_0(\eta)$ to $f(\eta)$ and $\theta(\eta)$. By using a Taylor series one may express that;

$$f(\eta,p) = f_0(\eta) + \sum_{m=1}^{\infty} f_m(\eta)p^m, \tag{27}$$

$$\theta(\eta, p) = \theta_0(\eta) + \sum_{m=1}^{\infty} \theta_m(\eta) p^m, \tag{28}$$

$$f_m(\eta) = \frac{1}{m!} \frac{\partial^m f(\eta; p)}{\partial \eta^m}\bigg|_{p=0}, \ \theta_m(\eta) = \frac{1}{m!} \frac{\partial^m \theta(\eta; p)}{\partial \eta^m}\bigg|_{p=0}. \tag{29}$$

The convergence of the series is strongly dependent upon $\hbar_f$ and $\hbar_\theta$. We select $\hbar_f$ and $\hbar_\theta$ in such a way that the series converge at $p = 1$ and hence;

$$f(\eta) = f_0(\eta) + \sum_{m=1}^{\infty} f_m(\eta), \tag{30}$$

$$\theta(\eta) = \theta_0(\eta) + \sum_{m=1}^{\infty} \theta_m(\eta). \tag{31}$$

**mth-order deformation equations**

The *m*th-order deformation equations are obtained by differentiating the Eqs. (23) - (25) *m* times with respect to *p* and then putting *p* = 0, we get;

$$L_f[f_m(\eta) - \chi_m f_{m-1}(\eta)] = \hbar_f \mathbf{R}_f^m(\eta), \tag{32}$$

$$L_\theta[\theta_m(\eta) - \chi_m \theta_{m-1}(\eta)] = \hbar_\theta \mathbf{R}_\theta^m(\eta), \tag{33}$$

$$f_m(0) = f_m'(0) - S_f f_m''(0) = f_m'(\infty) = 0, \ \ \theta_m(0) - S_T \theta_m'(0) = \theta_m(\infty) = 0, \tag{34}$$

$$\begin{aligned}\mathbf{R}_f^m(\eta) = {} & f_{m-1}'''(\eta) + \sum_{k=0}^{m-1}\left[ f_{m-1-k} f_k'' + \frac{1}{2}\eta\alpha^* f_{m-1}'' \right] + \sum_{k=0}^{m-1}[\alpha^* f_{m-1}' - f_{m-1}''] \\ & + \lambda^2(1-\chi_m) - \lambda\alpha^*(1-\chi_m),\end{aligned} \tag{35}$$

$$\mathbf{R}_\theta^m(\eta) = \theta_{m-1}'' + \Pr \sum_{k=0}^{m-1} \theta_{m-1-k}' f_k + \frac{1}{2} \Pr \alpha^* \eta \theta_{m-1}' + 2 \Pr \alpha^* \sum_{k=0}^{m-1} \theta_{m-1}, \tag{36}$$

$$\chi_m = \begin{bmatrix} 0, & m \le 1 \\ 1, & m > 1. \end{bmatrix} \tag{37}$$

Indicating $f_m^*(\eta)$ and $\theta_m^*(\eta)$ as the special solutions, we have the following series solutions.

$$f_m(\eta) = f_m^*(\eta) + C_1 + C_2 e^{\eta} + C_3 e^{-\eta}, \tag{38}$$
$$\theta_m(\eta) = \theta_m^*(\eta) + C_4 e^{\eta} + C_5 e^{-\eta}. \tag{39}$$

**Convergence of the derived solutions**

The solutions (30) and (31) consist of the nonzero auxiliary parameters $\hbar_f$ and $\hbar_\theta$. These parameters adjust and control the convergence of the homotopy solutions. The $\hbar-$ curves for 21st-order approximations are displayed for the permissible values of $\hbar_f$ and $\hbar_\theta$. Such values of $\hbar_f$ and $\hbar_\theta$ are $-1.5 \le \hbar_f \le -0.05$ and $-1.2 \le \hbar_\theta \le -0.5$ (see **Figure 1**). It is further shown that the series converges in the whole region of $\eta$ when $\hbar_f = -0.5$ and $\hbar_\theta = -1.10$.

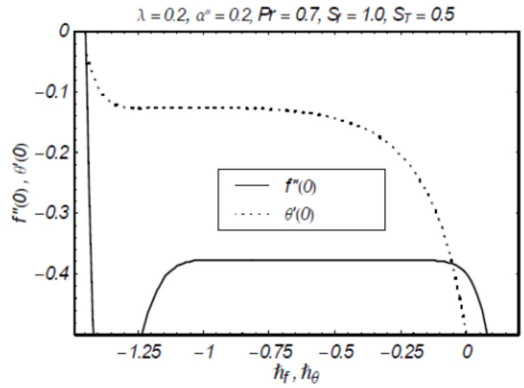


**Figure 1** $\hbar$-curves for the functions $f(\eta)$ and $\theta(\eta)$.

**Table 1** Convergence of the homotopy solution for different order of approximations when $\lambda = 0.2$, $\alpha^* = 0.1$, $\mathrm{Pr} = 0.7$, $S_f = 1.0$, $S_T = 0.5$ and $\hbar_f = -0.5$ and $\hbar_\theta = -1.10$.

| Order of approximation | -f′′(0) | -θ′(0) |
|---|---|---|
| 1 | 0.39125 | 0.43220 |
| 5 | 0.38494 | 0.26946 |
| 10 | 0.38507 | 0.24167 |
| 15 | 0.38508 | 0.23767 |
| 20 | 0.38508 | 0.23706 |
| 25 | 0.38508 | 0.23697 |
| 30 | 0.38508 | 0.23697 |
| 35 | 0.38508 | 0.23697 |

**Graphical results and discussion**

This section examines the effects of the slip parameter $S_f$, ratio of free stream and stretching velocity $\lambda$, unsteadiness parameter $\alpha^*$, Prandtl number Pr and thermal slip parameter $S_T$ on the velocity and temperature fields (**Figures 2 – 9**). The velocity profiles for different values of $S_f$ are plotted in **Figure 2**. It is seen that the boundary layer thickness decreases with increasing values of $S_f$. **Figure 3** shows the effects of $\lambda$ on $f'$. Clearly $f'$ is an increasing function of $\lambda$. **Figure**

**4** describes the effects of $\alpha^*$ on $f'$. Here $f'$ increases when $\alpha^*$ increases. The variation of Pr on $\theta$ is illustrated in **Figure 5**. The thermal boundary layer thickness decreases in view of an increase in Pr. **Figure 6** shows that the temperature field $\theta$ decreases for large values of $\lambda$. The behaviors of $\alpha^*$ and $S_f$ on temperature profiles are shown in the **Figures 7** and **8**. Both $\alpha^*$ and $S_f$ increase the temperature profile.

**Tables 2 - 4** are prepared for the numerical values of skin-friction coefficient and the local Nusselt number for different values of involved parameters of interest. From **Table 2** it is noticed that the magnitude of the skin-friction coefficient decreases for large values of $S_f$. This Table also indicates that for $\alpha^* = \lambda = 0$, the present solution has a good agreement with the exact analytical solution [21]. **Table 3** indicates that the effects of $\lambda$ and $S_f$ on skin-friction coefficient are similar. The local Nusselt number increases when the Prandtl number is increased while it decreases by increasing $S_T$ (**Table 4**).

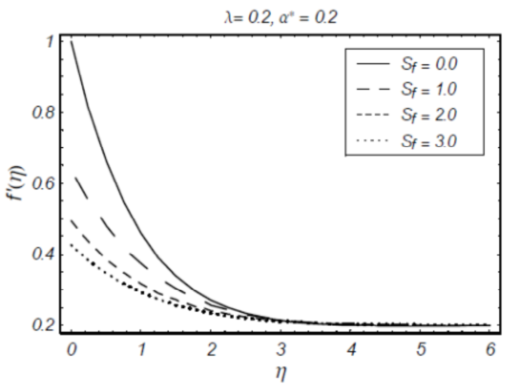


**Figure 2** Influence of $S_f$ on $f'(\eta)$.

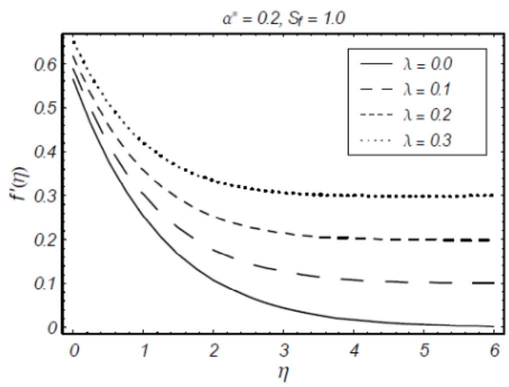


**Figure 3** Influence of $\lambda$ on $f'(\eta)$.

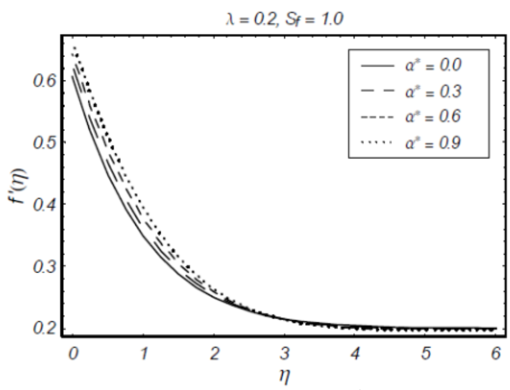


**Figure 4** Influence of $\alpha^*$ on $f'(\eta)$.

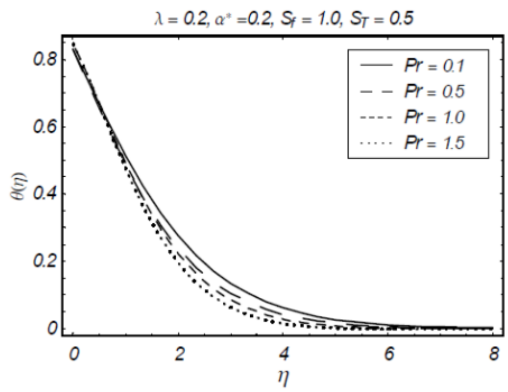


**Figure 5** Influence of Pr on $\theta(\eta)$.

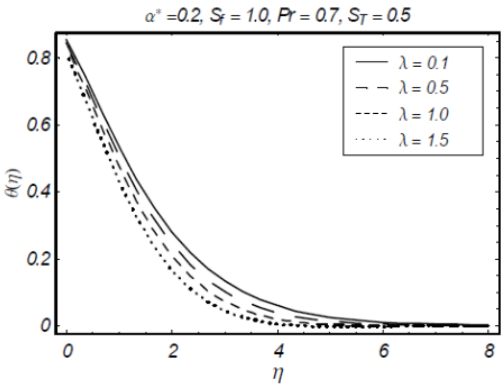


**Figure 6** Influence of $\lambda$ on $\theta(\eta)$.

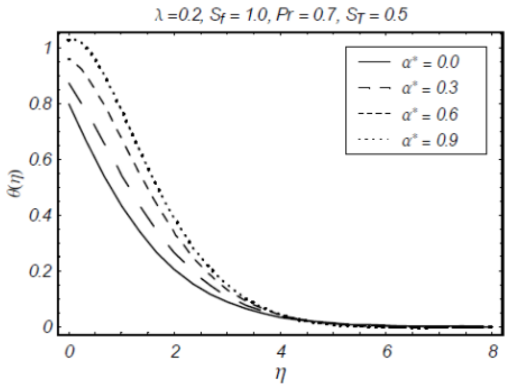


**Figure 7** Influence of $\alpha^*$ on $\theta(\eta)$.

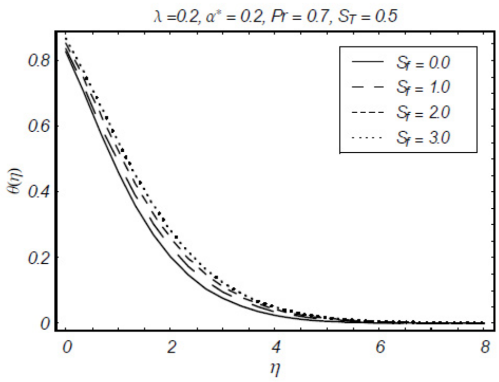


**Figure 8** Influence of $S_f$ on $\theta(\eta)$.

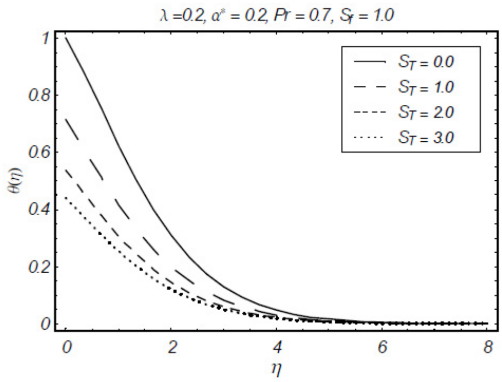


**Figure 9** Influence of $S_T$ on $\theta(\eta)$.

**Table 2** Comparison of $f'(0)$ and $-f''(0)$ for various values of $S_f$ at $h_f = -0.5$ with Andersson [21].

| $S_f$ | $f'(0)$ | | $-f''(0)$ | |
|---|---|---|---|---|
| | Andersson [21] | Present | Andersson [21] | Present |
| 0 | 1 | 1 | 1 | 1 |
| 0.1 | 0.9128 | 0.9127 | 0.8721 | 0.87208 |
| 0.2 | 0.8447 | 0.8447 | 0.7764 | 0.77637 |
| 0.5 | 0.7044 | 0.70440 | 0.5912 | 0.59119 |
| 1.0 | 0.5698 | 0.56984 | 0.4302 | 0.43016 |
| 2.0 | 0.4320 | 0.43204 | 0.2840 | 0.28398 |
| 5.0 | 0.2758 | 0.27799 | 0.1448 | 0.14484 |
| 10.0 | 0.1876 | 0.18756 | 0.0812 | 0.08124 |
| 20.0 | 0.1242 | 0.12421 | 0.0438 | 0.04378 |
| 50.0 | 0.0702 | 0.70223 | 0.0186 | 0.01858 |
| 100.0 | 0.0450 | 0.04524 | 0.0095 | 0.00955 |

**Table 3** Values of the skin-friction coefficient $\frac{1}{2}C_f \mathrm{Re}_x^{1/2}$ for different values of $\alpha^*$, $\lambda$ and $S_f$.

| $\alpha^*$ | $S_f$ | λ | $-(1/2)C_f Re_x^{1/2}$ |
|---|---|---|---|
| 0.0 | 1.0 | 0.2 | 0.3919 |
| 0.3 | | | 0.3705 |
| 0.5 | | | 0.3549 |
| 0.8 | | | 0.3296 |
| 0.1 | 0.0 | | 0.8940 |
| | 0.5 | | 0.5301 |
| | 1.5 | | 0.3046 |
| | 2.0 | | 0.2529 |
| | | 0.0 | 0.4178 |
| | | 0.3 | 0.3539 |
| | | 0.5 | 0.2725 |
| | | 0.8 | 0.1177 |

**Table 4** Values of local Nusselt number $Nu/\mathrm{Re}_x^{1/2}$ for parameters $S_T$, $S_f$ and Pr when $\lambda = 0.2$ and $\alpha^* = 0.1$.

| $S_T$ | $S_f$ | Pr | $-Nu/Re_x^{1/2}$ |
|---|---|---|---|
| 0.0 | 1.0 | 0.7 | 0.2690 |
| 0.5 | | | 0.2370 |
| 1.0 | | | 0.2121 |
| 2.0 | | | 0.1751 |
| 0.5 | 0.0 | | 0.3189 |
| | 0.5 | | 0.2659 |
| | 1.0 | | 0.2370 |
| | 2.0 | | 0.2039 |
| | | 0.5 | 0.2237 |
| | | 1.0 | 0.2936 |
| | | 1.5 | 0.3682 |
| | | 2.0 | 0.4275 |

## Concluding remarks

The slip effects on the flow of a viscous fluid with variable free stream velocity are considered. The reduced systems of coupled nonlinear ordinary differential equations are solved by the homotopy analysis method. The following main observations have been extracted from the presented analysis. Firstly, the effects of $S_f$ on velocity and temperature fields are opposite. The velocity decreases by increasing $S_f$ while temperature increases by increasing $S_f$. Secondly, the temperature field $\theta$ decreases by increasing the Prandtl number Pr. Thirdly, the velocity $f'$ and temperature $\theta$ increases by increasing $\alpha^*$. Finally, the thermal slip parameter $S_T$ decreases the temperature $\theta$.

## References

[1] BC Sakiadis. Boundary layer behaviour on continuous solid surfaces: I Boundary layer equations for two dimensional and axisymmetric flow. *AIChE. J.* 1961; **7**, 26-8.

[2] BC Sakiadis. Boundary layer behaviour on

continuous solid surfaces: II Boundary layer on a continuous flat surface. *AIChE. J.* 1961; **7**, 221-5.

[3] S Yao, T Fang and Y Zhong. Heat transfer of a generalized stretching/shrinking wall problem with convective boundary conditions. *Comm. Nonlinear Sci. Numer. Simulat.* 2011; **16**, 752-60.

[4] B Yao. Approximate analytical solution to the Falkner-Skan wedge flow with the permeable wall of uniform suction. *Comm. Nonlinear Sci. Numer. Simulat.* 2009; **14**, 3320-6.

[5] MM Rashidi and SAM Pour. Analytic approximate solutions for unsteady boundary-layer flow and heat transfer due to a stretching sheet by homotopy analysis method. *Nonlinear Anal. Model. Contr.* 2010; **15,** 83-95.

[6] S Nadeem, M Hussain and M Naz. MHD stagnation flow of a micropolar fluid through a porous medium. *Meccanica* 2010; **45**, 869-80.

[7] T Hayat, SA Shehzad, M Qasim and S Obaidat. Flow of a second grade fluid with convective boundary conditions. *Thermal Sci.* 2011; **15**, S253-S259.

[8] T Hayat, SA Shehzad, M Qasim and S Obaidat. Radiative flow of Jeffery fluid in a porous medium with power law heat flux and heat source. *Nuclear Eng. Design* 2012; **243**, 15-9.

[9] S Mukhopadhyay and HI Andersson. Effects of slip and heat transfer analysis of flow over an unsteady stretching surface. *Heat Mass Tran.* 2009; **45**, 1447-52.

[10] T Hayat, M Qasim and S Mesloub. MHD flow and heat transfer over permeable stretching sheet with slip conditions. *Int. J. Numer. Meth. Fluids* 2011; **66**, 963-75.

[11] PR Sharma and G Singh. Unsteady flow about a stagnation point on a stretching sheet in the presence of variable free stream. *Thammasat Int. J. Sci. Tech.* 2008; **13**, 11-6.

[12] J Zhu, LC Zheng and ZG Zhang. Effects of slip condition on MHD stagnation-point flow over a power law stretching sheet. *Appl. Math. Mech.* 2010; **31**, 439-48.

[13] T Fang, J Zhang and S Yao. Slip MHD viscous flow over a stretching sheet: An exact solution. *Comm. Nonlinear Sci. Numer. Simulat.* 2009; **14**, 3731-7.

[14] SJ Liao. Beyond perturbation: Introduction to homotopy analysis method. Chapman and Hall, CRC Press, Boca Raton, 2003.

[15] AK Alomari, MSM Noorani and R Nazar. Solutions of heat-like and wave-like equations with variable coefficients by means of the homotopy analysis method. *Chin. Phys. Lett.* 2008; **25**, 589-92.

[16] T Hayat and M Qasim. Influence of thermal radiation and joule heating on MHD flow of a Maxwell fluid in the presence of thermophoresis. *Int. J. Heat Mass Tran.* 2010; **53**, 4780-88.

[17] T Hayat, SA Shehzad, M Qasim and S Obaidat. Steady flow of Maxwell fluid with convective boundary conditions. *ZNA* 2011; **66**, 417-22.

[18] X Li. The application of homotopy analysis method to solve the coupled KdV equations. *Int. J. Nonlinear Sci.* 2011; **11**, 80-5.

[19] S Abbasbandy and A Shirzadi. Homotopy analysis method for a nonlinear chemistry problem. *Stud. Nonlinear Sci.* 2010; **1**, 127-32.

[20] MM Rashidi, AM Siddiqui and M Asadi. Application of homotopy analysis method to the unsteady squeezing flow of a second-grade fluid between circular plates. *Math. Probl. Eng.* 2010; **2010**, Article ID 706840.

[21] HI Andersson. Slip flow past a stretching surface. *Acta Mech.* 2002; **158**, 121-5.